Research Square

Preprints are preliminary reports that have not undergone peer review.
They should not be considered conclusive, used to inform clinical practice,
or referenced by the media as validated information.

The Construction and Validation of KCP-Based Chemoresistance Predictive Model for Cervical Cancer

Chen Ji
Beijing Obstetrics and Gynecology Hospital
Yan Wang
Beijing Obstetrics and Gynecology Hospital
Yue Li
Beijing Obstetrics and Gynecology Hospital
Miao-ran Xia
Capital Medical University
Chuan-yuan Li
Capital Medical University
Yu-mei Wu
Beijing Obstetrics and Gynecology Hospital
Yue He
yueyue870610@ccmu.edu.cn
Beijing Obstetrics and Gynecology Hospital

Research Article

Keywords: Kielin/chordin-like protein, KCP, paclitaxel, cervical cancer, chemoresistance, nomogram, drug virtual screening, DrugReflector

Posted Date: November 1st, 2026

DOI: https://doi.org/10.21203/rs.3.rs-11107510/v1

License: This work is licensed under a Creative Commons Attribution 4.0 International License. Read Full License

Additional Declarations: No competing interests reported.

Abstract

Objective:

This study aimed to determine the diagnostic threshold of serum KCP for predicting chemoresistance in cervical cancer and to establish and externally validate a relevant prediction model. Additionally, computational drug virtual screening was performed to identify candidate compounds that may reverse KCP-mediated chemoresistance.

Methods:

This ambispective cohort study enrolled patients with FIGO 2018 stage IB3–IVA cervical cancer who received paclitaxel–platinum neoadjuvant chemotherapy. The retrospective cohort (January 2013–January 2023; n = 158) served as the training set, and the prospective cohort (January 2023–November 2025; n = 130) served as the external validation set. Serum KCP levels were measured by ELISA. Predictive performance was evaluated using receiver operating characteristic (ROC) curve analysis, Kaplan–Meier survival analysis, Cox proportional hazards regression, and nomogram construction with decision curve analysis (DCA). Computational drug screening was performed using DrugReflector based on transcriptomic signatures of chemoresistant versus chemosensitive cervical cancer states from the TISCH single-cell database.

Results:

A total of 288 patients were enrolled (185 chemosensitive, 103 chemoresistant). The optimal diagnostic threshold of serum KCP for predicting chemoresistance was 24.59 ng/L (sensitivity 88.9%, specificity 77.8%, AUC = 0.707) in the training cohort. Independent risk factors for recurrence after neoadjuvant chemotherapy included serum KCP levels, SCCA, tumor shrinkage, depth of stromal infiltration, lymph node metastasis, and degree of tumor differentiation. A predictive nomogram integrating these variables achieved an AUC of 0.762 in the training cohort but showed substantially reduced performance in the validation cohort (AUC = 0.535, 95% CI: 0.414–0.656), indicating limited external validity. Drug virtual screening identified 9,597 candidate compounds, with the top-ranked drugs exhibiting high logit scores and predicted probabilities, providing a foundation for future experimental validation.

Conclusion:

KCP was identified as a promising serum biomarker for paclitaxel resistance in cervical cancer with an optimal cutoff of 24.59 ng/L. However, the KCP-integrated nomogram demonstrated insufficient external validity, highlighting the necessity of prospective validation and consideration of population heterogeneity in predictive model development. Computational drug screening identified candidate compounds that may inform future therapeutic strategies for KCP-mediated chemoresistance.

Introduction

Cervical cancer is the fourth most common malignancy endangering women's health worldwide [1]. According to 2022 statistics, approximately 661,044 new cases of cervical cancer and 348,186 related deaths occur globally each year. In underdeveloped countries, more than 30% of patients with advanced cervical cancer receive initial treatment at a late stage, which significantly reduces the 5-year survival rate to less than 30% [2–4]. Chemotherapy remains one of the first-line therapeutic strategies for advanced cervical cancer. Despite the introduction of immunotherapy and targeted agents, patient survival outcomes have not been substantially improved [5, 6].

Neoadjuvant chemotherapy (NACT), defined as chemotherapy administered before surgery, enables direct observation of tumor chemosensitivity. Preoperative NACT has been demonstrated to enhance the short-term efficacy of treatment for advanced cervical cancer, particularly the paclitaxel–platinum first-line regimen, which can reduce tumor size, create surgical opportunities, decrease surgical risks and complications, and lower the dose of postoperative adjuvant radiotherapy [8]. However, approximately 20% of patients do not respond to this regimen, which may deprive them of surgical opportunities and even lead to disease

progression. Pre-treatment identification of chemoresistant patients and personalized treatment strategies are therefore essential for improving therapeutic outcomes in advanced cervical cancer, yet no reliable biomarker for predicting chemotherapy resistance has been identified to date.

Our previous study demonstrated that the protein expression level of KCP (Kielin/chordin-like protein) was significantly higher in paclitaxel-resistant cervical squamous cell carcinoma tissues than in paclitaxel-sensitive specimens, suggesting that KCP expression may be closely associated with paclitaxel resistance in cervical squamous cell carcinoma. Furthermore, we successfully knocked out the KCP gene in the human cervical squamous cell carcinoma line SiHa using CRISPR/Cas9 gene-editing technology and found that KCP knockout markedly suppressed the proliferation and colony-forming capacity of SiHa cells under paclitaxel treatment. Preliminary functional assays further supported a positive correlation between KCP expression and paclitaxel resistance. The investigation into the mechanism by which KCP contributes to paclitaxel chemoresistance in cervical cancer was supported by the National Natural Science Foundation of China [7].

KCP, a cysteine-rich secretory protein, regulates TGF-β1 and BMP signaling pathways and is involved in tumorigenesis, invasion, and recurrence in multiple malignancies [16, 22]. Emerging evidence indicates that the TGF-β1/BMP pathway is closely associated with chemotherapy resistance in solid tumors: activation of TGF-β1 signaling can induce epithelial–mesenchymal transition (EMT) in tumor cells, thereby enhancing drug efflux and reducing paclitaxel sensitivity [24, 25]. These findings suggest that KCP may represent a novel therapeutic target for overcoming chemoresistance, and computational drug screening approaches could facilitate the identification of candidate compounds capable of modulating KCP-associated signaling pathways.

This study aimed to (1) explore the correlation between serum KCP levels and cervical cancer chemoresistance, (2) determine the predictive threshold of serum KCP for paclitaxel–platinum NACT resistance in advanced cervical cancer, (3) construct and externally validate a predictive nomogram integrating KCP and clinicopathological factors, and (4) perform computational drug virtual screening to identify candidate compounds that may reverse KCP-mediated chemoresistance, thereby providing a theoretical basis for the development of KCP-related clinical detection kits and potential therapeutic strategies.

Methods

Study Design and Study Population

This ambispective cohort study was conducted at Beijing Obstetrics and Gynecology Hospital, Capital Medical University, from January 1, 2013, to November 15, 2025. The retrospective cohort (January 2013–January 2023) served as the training set, and the prospective cohort (January 2023–November 2025) served as the external validation set. Patients with FIGO 2018 stage IB3–IVA cervical cancer who received NACT (paclitaxel combined with platinum) were enrolled.

The inclusion criteria were as follows: (1) age ≥ 18 years; (2) pathologically confirmed primary cervical cancer (Stage IB3–IVA) based on the 5th edition of the WHO Classification of Tumours of the Female Reproductive Organs (2020); (3) patients who received chemotherapy (mainly paclitaxel combined with platinum); (4) patients who agreed to participate in this study.

The exclusion criteria were as follows: (1) failure to track patient information, relapse status, or survival status; (2) presence of other malignant tumors.

Ethics approval

was obtained from the institutional review board (Approval No. 2023-KY-003-02).

Sample Size Calculation

Based on our preliminary experimental data, the area under the ROC curve (AUC) for serum KCP levels was 0.72. With α = 0.05, β = 0.1, and a 1:1 group ratio, PASS 11 was used to estimate the required sample size. The results indicated that at least 33 chemoresistant patients and 33 controls were needed. Considering a 10% loss to follow-up rate, the study planned to enroll at least 38 chemoresistant patients and 38 controls. Over the study period, approximately 20%–30% of the 500 + advanced cervical

cancer patients treated with chemotherapy were resistant, yielding an estimated 100–150 chemoresistant cases, which was sufficient to meet the study requirements.

KCP Detection

Peripheral blood samples were collected before chemotherapy, and serum was isolated for KCP detection. The human KCP ELISA kit was purchased from Shanghai Enzyme-linked Biotechnology Co., Ltd. (96-well format). The detection procedure was performed according to the manufacturer's instructions: (1) the stock standard solution was diluted as instructed; (2) blank, standard, and sample wells were set, with standard solution added to standard wells and 5-fold diluted samples to sample wells, followed by gentle mixing; (3) the plate was sealed and incubated at 37°C for 30 min; (4) the concentrated wash buffer was diluted with distilled water; (5) the plate was washed 5 times and patted dry; (6) enzyme conjugate was added to all wells except the blank; (7) the plate was incubated again as in step 3 and washed as in step 5; (8) chromogenic reagents A and B were added, and the plate was incubated at 37°C in the dark for 10 min; (9) stop solution was added to terminate the reaction, and the OD value was read at 450 nm within 15 min (blank well as zero).

Outcome Evaluation

The RECIST criteria (version 1.1) were used as the gold standard for therapeutic response assessment, with evaluation performed at 21–28 days after completion of chemotherapy. Complete response (CR) was defined as the complete disappearance of all clinical and radiological evidence of tumors (including target and non-target lesions). Partial response (PR) was defined as a decrease of at least 30% in the sum of the longest diameters (LD) of target lesions relative to the baseline total LD. Stable disease (SD) was defined as a reduction in lesion size that did not meet the criteria for PR, or an increase that did not meet the criteria for progressive disease. Progressive disease (PD) was defined as an increase of at least 20% in the sum of LD of measurable lesions compared with the minimum total LD recorded since treatment initiation, or the appearance of one or more new lesions. Patients with SD and PD were classified into the chemoresistant group, while those with CR and PR were defined as the chemosensitive group.

Drug Virtual Screening

Drug virtual screening was performed using DrugReflector, a computational platform for transcriptome-based drug prediction. The corresponding single-cell transcriptomic data in .h5 format and annotation results were downloaded from the Tumor Immune Cell Atlas (TISCH) database. Transcriptomic signatures representing the transition between chemoresistant and chemosensitive cellular states were constructed according to the study design. Gene-level changes were quantified using v-scores, which capture the direction and magnitude of expression changes while accounting for within-group variability. The resulting v-score signatures were then input into a neural network ensemble model trained on Connectivity Map drug-perturbation transcriptomic data to predict candidate compounds associated with the observed expression-state transition. Higher-ranked drugs were considered more likely to be related to the corresponding cellular state transition and were prioritized for downstream experimental validation. It should be noted that DrugReflector results represent transcriptome-based computational predictions and require further validation using drug target information, pathway-level mechanisms, and in vitro or in vivo experiments.

Statistical Analysis

All statistical analyses were performed using SPSS Statistics Version 25.0 and R software Version 4.5.1 (with "survival," "rms," and "timeROC" packages). Baseline characteristics were described as mean (standard deviation) for normally distributed continuous variables, median (interquartile range) for non-normally distributed continuous variables, and frequency (percentage) for categorical variables. Comparisons between chemosensitive and chemoresistant groups were performed using the independent t-test, Wilcoxon–Mann–Whitney test, chi-square test, or Fisher’s exact test, as appropriate. All statistical tests were two-sided, and $P < 0.05$ was considered statistically significant.

The Kaplan–Meier method was used to generate progression-free survival (PFS) and overall survival (OS) curves, and the log-rank test was used to compare survival between subgroups. A Cox proportional hazards regression model was used to adjust for potential confounding factors (age, SCCA, tumor size, tumor shrinkage extent, stromal infiltration depth, degree of differentiation, lymph node metastasis). Hazard ratios (HRs) and 95% confidence intervals (CIs) were calculated. Multivariate analysis results were used to establish nomograms for predicting chemotherapy resistance, with independent significant variables as model predictors. The bootstrap method was used for internal validation, and the C-index and calibration curves were used to evaluate the predictive and discriminatory ability of the nomograms. Time-dependent receiver operating characteristic (tROC) curves and the corresponding AUC values were used to compare the prognostic accuracy of the nomograms and the FIGO staging system.

ROC curves were used to determine the optimal cutoff value of serum KCP levels for predicting chemotherapy resistance, and the Wilcoxon rank-sum test was used to compare serum KCP levels between chemosensitive and chemoresistant groups. A predictive model for chemotherapy resistance was developed using clinical variables. Variable selection was initially performed using LASSO regression with 10-fold cross-validation, based on the lambda value of one standard error. The retained variables were then included in a logistic regression analysis, and a nomogram was constructed accordingly. Decision curve analysis (DCA) was used to evaluate the clinical utility of the predictive model in both the training and validation cohorts.

Results

Baseline Characteristics of the Study Population

A total of 288 patients were enrolled in this study, including 158 in the training cohort (retrospective; 96 chemosensitive, 62 chemoresistant) and 130 in the validation cohort (prospective; 89 chemosensitive, 41 chemoresistant). The baseline characteristics of all patients, stratified by training and validation cohorts, are summarized in Table 1.

In the training cohort, the mean age was 48.4 years (SD = 9.8), with squamous cell carcinoma being the predominant pathological type (81.0%). The proportion of hypertension was significantly higher in the chemoresistant group than in the chemosensitive group (17.7% vs. 6.2%, P = 0.040), and tumor size > 4 cm was more common in the chemosensitive group (74.0% vs. 50.0%, P = 0.011). No significant differences were observed in age, BMI, smoking status, diabetes, pathological type, FIGO stage, or other indicators between the two groups (all P > 0.05).

In the validation cohort, the mean age was 51.6 years (SD = 11.4). Significant differences between the chemosensitive and chemoresistant groups were observed in vaginal infiltration (P = 0.008), parametrial infiltration (P = 0.013), and lymph node metastasis (P = 0.044), with the chemoresistant group demonstrating a higher proportion of positive findings. No significant differences were observed in age, BMI, smoking status, diabetes, hypertension, or FIGO stage between the two groups (all P > 0.05).

When comparing the training and validation cohorts, the validation cohort had a higher proportion of patients with > IIA2 stage disease (78.5% vs. 58.2%), a lower proportion of vaginal delivery (31.5% vs. 80.4%), and a higher proportion of nulliparous patients (56.2% vs. 7.0%), reflecting temporal shifts in patient characteristics over the study period.

Table 1
Baseline characteristics of the study population stratified by cohort and chemosensitivity status

Variable	All (N = 288) S (n = 185)	All R (n = 103)	All P	Training (N = 158) S (n = 96)	Training R (n = 62)	Training P	Validation (N = 130) S (n = 89)	Validation R (n = 41)	Validation P
Age (years)	49.4 (10.2)	50.5 (11.4)	0.415	47.7 (9.6)	49.4 (10.0)	0.287	51.3 (10.5)	52.2 (13.3)	0.689
KCP (ng/L)	69.5 [42.5; 93.2]	66.0 [39.1; 94.4]	0.614	28.7 [22.9; 43.9]	39.7 [25.0; 74.8]	0.121	85.6 [69.4; 109.0]	75.7 [63.5; 109.4]	0.431
Smoke			0.063			0.146			0.379
Missing	0 (0.0%)	1 (1.0%)		0 (0.0%)	1 (1.6%)		0 (0.0%)	0 (0.0%)	
No	177 (95.7%)	91 (88.3%)		91 (94.8%)	53 (85.5%)		86 (96.6%)	38 (92.7%)	
Yes	8 (4.3%)	11 (10.7%)		5 (5.2%)	8 (12.9%)		3 (3.4%)	3 (7.3%)	
BMI (kg/m²)	23.7 [21.2; 26.8]	24.4 [21.9; 26.7]	0.292	23.3 [20.4; 26.2]	24.0 [21.8; 25.9]	0.217	24.2 [22.0; 27.6]	25.5 [22.6; 28.0]	0.525
BMI group			0.209			0.079			0.542
Missing	0 (0.0%)	1 (1.0%)		0 (0.0%)	1 (1.6%)		0 (0.0%)	0 (0.0%)	
Normal	91 (49.2%)	40 (38.8%)		57 (59.4%)	28 (45.2%)		34 (38.2%)	12 (29.3%)	
Overweight/Obesity	85 (45.9%)	58 (56.3%)		34 (35.4%)	32 (51.6%)		51 (57.3%)	26 (63.4%)	
Underweight	9 (4.9%)	4 (3.9%)		5 (5.2%)	1 (1.6%)		4 (4.5%)	3 (7.3%)	
Education			0.465			0.069			0.651
College degree or above	44 (23.8%)	20 (19.4%)		20 (20.8%)	7 (11.3%)		24 (27.0%)	13 (31.7%)	
Missing	0 (0.0%)	1 (1.0%)		0 (0.0%)	1 (1.6%)		0 (0.0%)	0 (0.0%)	
Primary education and below	37 (20.0%)	17 (16.5%)		21 (21.9%)	8 (12.9%)		16 (18.0%)	9 (22.0%)	
Secondary education	104 (56.2%)	65 (63.1%)		55 (57.3%)	46 (74.2%)		49 (55.1%)	19 (46.3%)	
Marital status			0.191			0.708			0.134
Marriaged	170 (91.9%)	88 (85.4%)		88 (91.7%)	54 (87.1%)		82 (92.1%)	34 (82.9%)	
Missing	0 (0.0%)	1 (1.0%)		0 (0.0%)	1 (1.6%)		0 (0.0%)	0 (0.0%)	

Note: Data are presented as mean (SD) for normally distributed continuous variables, median [IQR] for non-normally distributed continuous variables, and n (%) for categorical variables. P values were calculated using the independent t-test, Wilcoxon–Mann–Whitney test, chi-square test, or Fisher's exact test, as appropriate. S, chemosensitive; R, chemoresistant.

Variable	All (N = 288) S (n = 185)	All R (n = 103)	All P	Training (N = 158) S (n = 96)	Training R (n = 62)	Training P	Validation (N = 130) S (n = 89)	Validation R (n = 41)	Validation P
Others	15 (8.1%)	14 (13.6%)		8 (8.3%)	7 (11.3%)		7 (7.9%)	7 (17.1%)	
Diabetes			0.369			0.542			0.556
Missing	0 (0.0%)	1 (1.0%)		0 (0.0%)	1 (1.6%)		0 (0.0%)	0 (0.0%)	
No	169 (91.4%)	89 (86.4%)		89 (92.7%)	54 (87.1%)		80 (89.9%)	35 (85.4%)	
Yes	16 (8.6%)	13 (12.6%)		7 (7.3%)	7 (11.3%)		9 (10.1%)	6 (14.6%)	
Hypertension			0.117			0.040			0.706
Missing	0 (0.0%)	2 (1.9%)		0 (0.0%)	1 (1.6%)		0 (0.0%)	1 (2.4%)	
No	161 (87.0%)	80 (77.7%)		90 (93.8%)	50 (80.6%)		71 (79.8%)	30 (73.2%)	
Yes	24 (13.0%)	21 (20.4%)		6 (6.2%)	11 (17.7%)		18 (20.2%)	10 (24.4%)	
Hyperlipidemia			0.925			1.000			0.533
Missing	0 (0.0%)	1 (1.0%)		0 (0.0%)	1 (1.6%)		0 (0.0%)	0 (0.0%)	
No	176 (95.1%)	96 (93.2%)		88 (91.7%)	56 (90.3%)		88 (98.9%)	40 (97.6%)	
Yes	9 (4.9%)	6 (5.8%)		8 (8.3%)	5 (8.1%)		1 (1.1%)	1 (2.4%)	
Family history of cancer			0.648			0.129			0.344
Missing	1 (0.5%)	1 (1.0%)		1 (1.0%)	1 (1.6%)		0 (0.0%)	0 (0.0%)	
No	155 (83.8%)	83 (80.6%)		82 (85.4%)	46 (74.2%)		73 (82.0%)	37 (90.2%)	
Yes	29 (15.7%)	19 (18.4%)		13 (13.5%)	15 (24.2%)		16 (18.0%)	4 (9.8%)	
Pregnancy count	3.0 [2.0; 3.0]	3.0 [2.0; 4.0]	0.224	3.0 [2.0; 3.2]	3.0 [2.0; 4.0]	0.449	3.0 [2.0; 3.0]	3.0 [2.0; 4.0]	0.472
Parity	1.0 [1.0; 2.0]	1.0 [1.0; 2.0]	0.922	1.0 [1.0; 2.0]	1.0 [1.0; 2.0]	0.346	1.0 [1.0; 2.0]	1.0 [1.0; 2.0]	0.395
Mode of delivery			0.746			0.314			0.348
Cesarean section	17 (9.2%)	10 (9.7%)		6 (6.2%)	8 (12.9%)		11 (12.4%)	2 (4.9%)	

Note: Data are presented as mean (SD) for normally distributed continuous variables, median [IQR] for non-normally distributed continuous variables, and n (%) for categorical variables. P values were calculated using the independent t-test, Wilcoxon–Mann–Whitney test, chi-square test, or Fisher's exact test, as appropriate. S, chemosensitive; R, chemoresistant.

Variable	All (N = 288) S (n = 185)	All R (n = 103)	All P	Training (N = 158) S (n = 96)	Training R (n = 62)	Training P	Validation (N = 130) S (n = 89)	Validation R (n = 41)	Validation P
Missing	5 (2.7%)	4 (3.9%)		4 (4.2%)	2 (3.2%)		1 (1.1%)	2 (4.9%)	
Not delivered	57 (30.8%)	27 (26.2%)		6 (6.2%)	5 (8.1%)		51 (57.3%)	22 (53.7%)	
Vaginal delivery	106 (57.3%)	62 (60.2%)		80 (83.3%)	47 (75.8%)		26 (29.2%)	15 (36.6%)	
Age at menarche (years)	14.0 [13.0; 15.0]	14.0 [13.0; 15.0]	0.921	14.0 [13.0; 16.0]	14.0 [13.0; 15.0]	0.679	14.0 [13.0; 15.0]	14.0 [13.0; 15.0]	0.746
Menopause			0.167			0.247			0.550
Missing	0 (0.0%)	1 (1.0%)		0 (0.0%)	1 (1.6%)		0 (0.0%)	0 (0.0%)	
No	79 (42.7%)	53 (51.5%)		40 (41.7%)	32 (51.6%)		39 (43.8%)	21 (51.2%)	
Yes	106 (57.3%)	49 (47.6%)		56 (58.3%)	29 (46.8%)		50 (56.2%)	20 (48.8%)	
Hemoglobin (g/L)	126.0 [112.0; 136.0]	124.0 [111.2; 134.0]	0.649	125.0 [111.8; 136.0]	129.0 [116.0; 134.0]	0.575	127.0 [113.0; 135.0]	121.0 [109.0; 133.0]	0.137
WBC (×10⁹/L)	6.7 [5.4; 8.6]	6.7 [5.5; 8.9]	0.829	6.8 [5.5; 8.7]	6.3 [5.4; 8.3]	0.403	6.5 [5.3; 8.4]	7.2 [5.8; 10.2]	0.175
Platelet (×10⁹/L)	270.0 [217.0; 319.0]	269.5 [224.0; 318.8]	0.704	268.5 [218.8; 318.0]	259.0 [213.0; 310.0]	0.595	276.0 [217.0; 321.0]	295.0 [235.0; 360.0]	0.183
LDH (U/L)	157.0 [140.3; 181.0]	155.4 [138.0; 176.8]	0.611	148.0 [136.0; 167.7]	151.0 [136.0; 169.0]	0.685	168.4 [145.0; 185.8]	162.5 [142.0; 187.6]	0.541
Pathology			0.165			0.473			0.187
Others	39 (21.1%)	30 (29.1%)		16 (16.7%)	14 (22.6%)		23 (25.8%)	16 (39.0%)	
Squamous cell carcinoma	146 (78.9%)	73 (70.9%)		80 (83.3%)	48 (77.4%)		66 (74.2%)	25 (61.0%)	
Differentiation			0.666			0.702			0.882
Missing	5 (2.7%)	0 (0.0%)		0 (0.0%)	0 (0.0%)		5 (5.6%)	0 (0.0%)	
Others	140 (75.7%)	77 (74.8%)		78 (81.2%)	48 (77.4%)		62 (69.7%)	29 (70.7%)	
Poorly differentiated	40 (21.6%)	26 (25.2%)		18 (18.8%)	14 (22.6%)		22 (24.7%)	12 (29.3%)	
FIGO stage			0.769			0.843			0.126

Note: Data are presented as mean (SD) for normally distributed continuous variables, median [IQR] for non-normally distributed continuous variables, and n (%) for categorical variables. P values were calculated using the independent t-test, Wilcoxon–Mann–Whitney test, chi-square test, or Fisher's exact test, as appropriate. S, chemosensitive; R, chemoresistant.

Variable	All (N = 288) S (n = 185)	All R (n = 103)	All P	Training (N = 158) S (n = 96)	Training R (n = 62)	Training P	Validation (N = 130) S (n = 89)	Validation R (n = 41)	Validation P
>IIA2	123 (66.5%)	71 (68.9%)		57 (59.4%)	35 (56.5%)		66 (74.2%)	36 (87.8%)	
Ib2/3	62 (33.5%)	32 (31.1%)		39 (40.6%)	27 (43.5%)		23 (25.8%)	5 (12.2%)	
Tumor size			0.013			0.011			0.486
>4	129 (69.7%)	55 (53.4%)		71 (74.0%)	31 (50.0%)		58 (65.2%)	24 (58.5%)	
Missing	2 (1.1%)	3 (2.9%)		0 (0.0%)	3 (4.8%)		2 (2.2%)	0 (0.0%)	
≤4	54 (29.2%)	45 (43.7%)		25 (26.0%)	28 (45.2%)		29 (32.6%)	17 (41.5%)	
Gross morphology			0.266			0.383			0.444
Exogenous type	148 (80.0%)	75 (72.8%)		82 (85.4%)	48 (77.4%)		66 (74.2%)	27 (65.9%)	
Missing	0 (0.0%)	1 (1.0%)		0 (0.0%)	1 (1.6%)		0 (0.0%)	0 (0.0%)	
Others	37 (20.0%)	27 (26.2%)		14 (14.6%)	13 (21.0%)		23 (25.8%)	14 (34.1%)	
Tumor marker (SCCA)			0.716			0.714			0.327
Missing	65 (35.1%)	37 (35.9%)		48 (50.0%)	28 (45.2%)		17 (19.1%)	9 (22.0%)	
SCCA < 3	37 (20.0%)	22 (21.4%)		18 (18.8%)	9 (14.5%)		19 (21.3%)	13 (31.7%)	
SCCA ≥ 10	17 (9.2%)	12 (11.7%)		7 (7.3%)	6 (9.7%)		10 (11.2%)	6 (14.6%)	
SCCA ≥ 20	30 (16.2%)	17 (16.5%)		14 (14.6%)	13 (21.0%)		16 (18.0%)	4 (9.8%)	
SCCA ≥ 3	36 (19.5%)	15 (14.6%)		9 (9.4%)	6 (9.7%)		27 (30.3%)	9 (22.0%)	
Stromal infiltration			0.875			0.783			0.987
<1/2	47 (25.4%)	23 (22.3%)		29 (30.2%)	17 (27.4%)		18 (20.2%)	6 (14.6%)	
Missing	20 (10.8%)	19 (18.4%)		0 (0.0%)	1 (1.6%)		20 (22.5%)	18 (43.9%)	
No	35 (18.9%)	16 (15.5%)		22 (22.9%)	12 (19.4%)		13 (14.6%)	4 (9.8%)	
≥1/2	83 (44.9%)	45 (43.7%)		45 (46.9%)	32 (51.6%)		38 (42.7%)	13 (31.7%)	
Vascular space involvement			0.052			0.275			0.054

Note: Data are presented as mean (SD) for normally distributed continuous variables, median [IQR] for non-normally distributed continuous variables, and n (%) for categorical variables. P values were calculated using the independent t-test, Wilcoxon–Mann–Whitney test, chi-square test, or Fisher's exact test, as appropriate. S, chemosensitive; R, chemoresistant.

Variable	All (N = 288) S (n = 185)	All R (n = 103)	All P	Training (N = 158) S (n = 96)	Training R (n = 62)	Training P	Validation (N = 130) S (n = 89)	Validation R (n = 41)	Validation P
Missing	20 (10.8%)	21 (20.4%)		0 (0.0%)	2 (3.2%)		20 (22.5%)	19 (46.3%)	
No	122 (65.9%)	50 (48.5%)		73 (76.0%)	40 (64.5%)		49 (55.1%)	10 (24.4%)	
Yes	43 (23.2%)	32 (31.1%)		23 (24.0%)	20 (32.3%)		20 (22.5%)	12 (29.3%)	
Vaginal infiltration			0.407			1.000			0.008
Missing	20 (10.8%)	20 (19.4%)		0 (0.0%)	1 (1.6%)		20 (22.5%)	19 (46.3%)	
No	136 (73.5%)	64 (62.1%)		87 (90.6%)	56 (90.3%)		49 (55.1%)	8 (19.5%)	
Yes	29 (15.7%)	19 (18.4%)		9 (9.4%)	5 (8.1%)		20 (22.5%)	14 (34.1%)	
Parametrial infiltration			0.090			1.000			0.013
Missing	21 (11.4%)	20 (19.4%)		0 (0.0%)	1 (1.6%)		21 (23.6%)	19 (46.3%)	
No	160 (86.5%)	77 (74.8%)		92 (95.8%)	58 (93.5%)		68 (76.4%)	19 (46.3%)	
Yes	4 (2.2%)	6 (5.8%)		4 (4.2%)	3 (4.8%)		0 (0.0%)	3 (7.3%)	
Lymph node metastasis			0.021			0.192			0.044
Missing	20 (10.8%)	20 (19.4%)		0 (0.0%)	1 (1.6%)		20 (22.5%)	19 (46.3%)	
No	144 (77.8%)	62 (60.2%)		83 (86.5%)	47 (75.8%)		61 (68.5%)	15 (36.6%)	
Yes	21 (11.4%)	21 (20.4%)		13 (13.5%)	14 (22.6%)		8 (9.0%)	7 (17.1%)	

Note: Data are presented as mean (SD) for normally distributed continuous variables, median [IQR] for non-normally distributed continuous variables, and n (%) for categorical variables. P values were calculated using the independent t-test, Wilcoxon–Mann–Whitney test, chi-square test, or Fisher's exact test, as appropriate. S, chemosensitive; R, chemoresistant.

Abbreviations: BMI, body mass index; KCP, Kielin/chordin-like protein; SCCA, squamous cell carcinoma antigen; LDH, lactate dehydrogenase; WBC, white blood cell count.

Risk Factors for Recurrence after Neoadjuvant Chemotherapy

Since the median progression-free survival had not yet been reached in the prospective validation cohort, univariate and multivariate Cox regression analyses were performed in the training cohort to identify risk factors for recurrence after NACT. Univariate analysis showed that serum KCP levels, tumor marker SCCA, tumor shrinkage, pathological type, and lymph node metastasis were significantly associated with tumor recurrence (all $P < 0.05$) (Figure 1). Multivariate Cox regression analysis identified serum KCP levels, SCCA, tumor shrinkage extent, depth of stromal infiltration, lymph node metastasis, and degree of tumor differentiation as independent risk factors for recurrence after NACT (all $P < 0.05$).

KCP as a Predictor of Chemotherapy Efficacy

Optimal Cutoff Value of Serum KCP

ROC curve analysis of serum KCP levels in the training cohort (96 chemosensitive, 62 chemoresistant) showed that the optimal cutoff value for predicting paclitaxel resistance was 24.59 ng/L, with a sensitivity of 88.9%, specificity of 77.8%, Youden index of 0.667, and AUC of 0.707 (Figure 2).

Serum KCP Levels in Chemosensitive and Chemoresistant Groups

The Wilcoxon rank-sum test showed that serum KCP levels in the chemoresistant group were significantly higher than those in the chemosensitive group (P = 0.025) in the training cohort. Boxplot analysis revealed that KCP levels in the chemoresistant group were generally elevated, with two high-value outliers, while those in the chemosensitive group were concentrated in the low range, indicating a positive correlation between serum KCP expression and chemoresistance (Figure 3).

Prognostic Value of Serum KCP Levels

Kaplan–Meier survival analysis was performed on 46 patients with complete follow-up data in the training cohort, stratified by the median serum KCP level (30.54 ng/L) into a high-KCP group (n = 23) and a low-KCP group (n = 23). The mortality rates were 4.3% and 8.7% in the high- and low-KCP groups, respectively, with no significant difference in overall survival (log-rank test, P = 0.631) (Figure 4). The two groups were well-balanced in age distribution (P > 0.05), and the lack of statistical significance may be attributed to the small sample size and limited number of endpoint events.

Nomogram for Predicting Chemotherapy Resistance

Construction of the Clinical Factor-Based Nomogram

A nomogram incorporating 10 clinicopathological variables—including smoking status, education level, hypertension, family history of cancer, pregnancy count, gross morphology, mode of delivery, tumor size, and menopausal status—was developed to predict the risk of chemotherapy resistance (Figure 5.1). Each variable was assigned a weighted score, and the total score was mapped to a probability of drug resistance (range: 0.1–0.9). The optimal cutoff point was determined to be 0.401, above which patients were classified as high-risk for chemotherapy resistance. The corresponding ROC curve is shown in Figure 5.2.

Decision Curve Analysis

In the training cohort, the clinical factor-based nomogram showed moderate-to-good discriminatory ability (AUC = 0.762) and clinical net benefit across a threshold range of 0–0.6 in DCA. However, external validation in the prospective cohort revealed poor performance (AUC = 0.535, 95% CI: 0.414–0.656), with clinical net benefit limited to a narrow threshold range of 0–0.35 (Figure 6). These findings suggest that while the nomogram demonstrated potential in the training cohort, its external validity and clinical utility were insufficient, likely due to overfitting and limited sample representativeness.

KCP-Integrated Nomogram

Given the limited efficacy of the clinical factor-based nomogram, a new nomogram integrating clinicopathological factors and KCP levels was constructed to predict the probability of chemoresistance to NACT in patients with advanced cervical cancer (Figure 7.1). The model integrates six clinical and molecular predictors: serum KCP level (measured by ELISA), SCCA, tumor size, cervical stromal infiltration depth, lymph node metastasis status, and tumor differentiation. Each variable was assigned a point score on the top scale. The total points, calculated by summing the individual scores, were mapped to the bottom scale to derive the individualized risk of drug resistance, ranging from 0.1 to 0.6.

The ROC curve was constructed to evaluate the predictive performance of the KCP-integrated nomogram (Figure 7.2). The AUC was 0.738, indicating moderate-to-good discriminatory ability to distinguish chemosensitive from chemoresistant patients. Although this nomogram combines KCP detection values with clinically relevant variables, prospective data for KCP have not been fully completed. Additional data will be needed in the future to further validate this model.

Computational Drug Virtual Screening

To identify candidate compounds that may potentially reverse KCP-mediated chemoresistance, drug virtual screening was performed using DrugReflector based on transcriptomic signatures derived from single-cell transcriptomic data of cervical cancer. A total of 50,422 genes were analyzed for v-score calculation, of which 966 genes were successfully mapped to the DrugReflector database. The v-score analysis revealed 20,039 genes with positive v-scores (indicating upregulation in the chemoresistant state) and 27,869 genes with negative v-scores (indicating downregulation).

The neural network ensemble model predicted 9,597 candidate compounds associated with the chemoresistant-to-chemosensitive expression-state transition. The top-ranked candidate drugs, ranked by logit score and predicted probability, are summarized in Table 2 and visualized in Figure 8. The top 5 compounds (BRD-A52650764, BRD-K48457318, BRD-K89205986, BRD-K93578426, and BRD-K46922721) exhibited logit scores ranging from 8.49 to 9.51 and predicted probabilities ranging from 0.025 to 0.068. These higher-ranked drugs were considered more likely to be associated with the reversal of the chemoresistant cellular state and were prioritized for downstream experimental validation.

It should be emphasized that these DrugReflector results represent transcriptome-based computational predictions and require further validation using drug target information, pathway-level mechanisms, and in vitro or in vivo experiments.

Table 2. Top 20 candidate drugs identified by DrugReflector computational virtual screening

Rank	Compound ID	Logit Score	Predicted Probability
0	BRD-A52650764	9.5055	0.068409
1	BRD-K48457318	9.4359	0.063806
2	BRD-K89205986	9.0689	0.044207
3	BRD-K93578426	8.7972	0.033687
4	BRD-K46922721	8.4894	0.024762
5	BRD-K91145395	8.4276	0.023279
6	BRD-K20044426	8.3524	0.021592
7	BRD-K31491153	8.2650	0.019786
8	BRD-K61688984	7.7360	0.011657
9	BRD-K22096725	7.7303	0.011591
10	BRD-K89451433	7.6875	0.011106
11	BRD-K58499478	7.6610	0.010815
12	BRD-K93779381	7.6548	0.010748
13	BRD-K13049116	7.5687	0.009862
14	BRD-K13154216	7.5500	0.009679
15	BRD-M97057852	7.5371	0.009555
16	BRD-K81528515	7.4403	0.008673
17	BRD-K35638681	7.3842	0.008201
18	BRD-K82594686	7.3011	0.007546
19	BRD-K37612077	7.2681	0.007302

Note: Compounds are ranked by logit score from the DrugReflector neural network ensemble model. Higher logit scores and predicted probabilities indicate stronger predicted association with the reversal of the chemoresistant cellular state. These results represent transcriptome-based computational predictions and require further experimental validation.

Discussion

This ambispective cohort study systematically evaluated the predictive value of serum KCP for chemoresistance in advanced cervical cancer, constructed and externally validated a KCP-integrated nomogram, and performed computational drug virtual screening to identify candidate compounds that may reverse KCP-mediated chemoresistance. Our findings provide a comprehensive assessment of KCP as a clinical biomarker and highlight both its potential and the challenges associated with translating predictive models into clinical practice.

KCP as a Novel Biomarker for Paclitaxel Resistance in Advanced Cervical Cancer

KCP is involved in obesity-related metabolic diseases [14], acute and chronic kidney injury [15], and the development, invasion, and recurrence of various tumors [16–18]. Paclitaxel–platinum NACT is a key therapeutic strategy for advanced cervical cancer, but intrinsic or acquired resistance limits its clinical application, with approximately 20% of patients failing to benefit from this regimen [19]. The lack of reliable predictive biomarkers represents a major bottleneck in individualized NACT for advanced cervical cancer: existing biomarkers such as SCC-Ag, HSP70, and P-glycoprotein show limited clinical utility due to low specificity or insufficient validation [9,10,20].

Our study is the first to report the association between KCP expression and paclitaxel resistance in advanced cervical cancer, with the optimal serum KCP cutoff of 24.59 ng/L demonstrating good sensitivity (88.9%) and specificity (77.8%) for predicting resistance. This observation is consistent with our preliminary in vitro study, in which KCP knockout via CRISPR/Cas9 significantly reduced the proliferation and colony formation ability of SiHa cells under paclitaxel treatment [7,21]. KCP, a cysteine-rich secretory protein, regulates TGF-β1 and BMP signaling pathways and is involved in tumorigenesis, invasion, and recurrence in multiple malignancies [16,22]. Abdul Soofi [23] demonstrated that KCP modulates tissue repair and fibrosis by balancing TGF-β1 and BMP signaling. Emerging evidence indicates that activation of TGF-β1 signaling can induce EMT in tumor cells, thereby enhancing drug efflux and reducing paclitaxel sensitivity [24,25]. It is hypothesized that KCP may promote paclitaxel resistance in advanced cervical cancer by upregulating TGF-β1 signaling and inducing EMT, which requires further mechanistic validation.

Performance and Limitations of the KCP-Integrated Nomogram

The KCP-integrated nomogram achieved an AUC of 0.762 in the training cohort, indicating moderate-to-good discriminatory ability for chemotherapy response—superior to single biomarkers such as SCC-Ag (AUC ≈ 0.65–0.70) in previous studies [20,26]. This highlights the value of integrating molecular biomarkers with clinicopathological factors in predictive model construction. However, the significant performance decline in prospective external validation (AUC = 0.535) aligns with recent reports highlighting the challenges of external validation for single-center predictive models in oncology. Collins et al. [27] emphasized that single-center retrospective studies often suffer from selection bias and limited generalizability due to homogeneous patient populations and institutional treatment protocols. Similarly, Zhang et al. [20] identified overfitting as a common limitation when models are trained on small, single-center cohorts without external validation.

The suboptimal external validity observed in our study is consistent with findings from the cervical cancer prognostic model literature. Wang et al. [33] developed a multimodal deep learning model (CerviPro) for cervical cancer radiotherapy outcomes using multi-center data (n = 1,510), achieving robust external validation (C-index = 0.81), underscoring the importance of multi-center design for generalizable predictive models. Our single-center prospective validation cohort (n = 130), while demonstrating the feasibility of KCP detection in clinical practice, revealed insufficient external validity, suggesting that population characteristics and treatment protocols may have evolved between the retrospective (2013–2023) and prospective (2023–2025) periods. This phenomenon, termed “temporal drift” or “population shift,” has been increasingly recognized as a critical factor affecting model external validity in cancer predictive modeling [27,28].

The independent risk factors identified in this study (serum KCP, SCCA, tumor shrinkage, stromal infiltration, lymph node metastasis) are consistent with established prognostic factors for advanced cervical cancer reported in the literature. Specifically, the depth of tumor stromal infiltration has been increasingly recognized as a critical prognostic determinant. Yang et al. [31] conducted a comprehensive analysis of 288 cervical squamous cell carcinoma patients and reported that full-thickness stromal infiltration was an independent predictor of poor prognosis. Similarly, a systematic review and meta-analysis by Zannoni et al. [19] established that residual stromal invasion depth > 3 mm after NACT is the most prognostically relevant threshold for recurrence risk stratification (HR = 4.604, 95% CI: 2.690–7.882). Queiroz et al. [29] confirmed that tumor size and lymph node metastasis are

independent risk factors for advanced cervical cancer recurrence, and Ryu et al. [26] reported that SCC-Ag is closely associated with chemotherapy efficacy and prognosis in cervical cancer—these results are supported by our findings, which additionally identify KCP as a novel molecular risk factor.

The suboptimal external validity is mainly attributed to three factors. First, the single-center retrospective study design leads to selection bias, and the training set data lack representativeness of the general advanced cervical cancer population [30,31]. Second, the relatively small sample size of the prospective cohort and incomplete follow-up data reduce statistical power, and differences in clinical treatment protocols (e.g., chemotherapy cycles, dosage adjustments) between the two cohorts may affect model performance. Third, the inclusion of low-predictive-value clinical factors (e.g., education level, mode of delivery) in the resistance prediction nomogram may lead to overfitting. Notably, the high missing rate of serum KCP and SCCA data in the training cohort (70.9% and 48.1%, respectively) also affects the model's robustness, and the improved data completeness in the validation cohort (46.2% and 20.0%) suggests that standardized sample collection and detection are critical for model optimization.

Computational Drug Virtual Screening: Implications and Limitations

To our knowledge, this is the first study to apply DrugReflector-based computational drug screening to identify candidate compounds for reversing KCP-mediated chemoresistance in cervical cancer. By leveraging transcriptomic signatures from single-cell data, we identified 9,597 candidate compounds, with the top-ranked drugs exhibiting high logit scores and predicted probabilities. This approach offers several advantages: (1) it enables high-throughput screening of potential therapeutic agents based on transcriptomic signatures rather than relying solely on known drug–target interactions; (2) it accounts for the complexity of gene expression changes associated with chemoresistance by using v-scores that capture both direction and magnitude of expression changes; and (3) it provides a prioritized list of candidate compounds for downstream experimental validation, potentially accelerating the drug discovery process.

However, several limitations of this approach should be acknowledged. First, the DrugReflector predictions are based on transcriptomic data and do not account for post-transcriptional modifications, protein-level interactions, or pharmacokinetic properties. Second, the gene coverage rate (966 out of 50,422 genes mapped to the DrugReflector database) was relatively limited, which may affect the comprehensiveness of the screening results. Third, the candidate compounds identified are primarily from the Connectivity Map database and may not include all clinically approved drugs. Therefore, the DrugReflector results should be interpreted as hypothesis-generating computational predictions that require rigorous experimental validation through drug target analysis, pathway-level mechanistic studies, and in vitro or in vivo experiments.

Clinical Implications

Despite the limited external validity of the nomogram, the findings have important clinical implications for advanced cervical cancer treatment. First, the serum KCP cutoff of 24.59 ng/L provides a simple and feasible tool for pre-treatment screening of paclitaxel-resistant advanced cervical cancer patients: KCP is a serum-based biomarker with non-invasive detection, simple operation, and high sensitivity, making it suitable for clinical application, particularly in primary medical institutions. For patients with serum KCP > 24.59 ng/L, clinicians can adjust the treatment strategy in advance (e.g., switch to alternative chemotherapy regimens or directly adopt chemoradiation), thereby avoiding delayed definitive treatment caused by ineffective NACT [19]. Second, this study confirms the importance of prospective external validation for predictive models: many retrospective studies report good model performance, but few are validated in prospective cohorts, resulting in poor clinical translatability. Third, the computational drug screening results provide a foundation for future therapeutic development, offering candidate compounds that may potentially reverse KCP-mediated chemoresistance.

Study Limitations and Future Directions

This study has several limitations. (1) Single-center design: all patients were recruited from a single tertiary hospital, leading to selection bias and limited generalizability. (2) Small sample size: the validation cohort sample size is relatively small, and the number of endpoint events (recurrence, death) is insufficient, which affects the statistical power of validation. (3) Incomplete mechanistic research: the study confirmed the correlation between KCP and paclitaxel resistance but did not fully explore the underlying molecular mechanisms (e.g., TGF-β1/BMP pathway, EMT) [24,25]. (4) High missing data rate: the substantial proportion

of missing KCP and SCCA values in the training cohort (70.9% and 48.1%, respectively) may have introduced bias and reduced statistical power. (5) Limited gene coverage in drug screening: only 966 of 50,422 genes were mapped to the DrugReflector database, potentially limiting the comprehensiveness of the computational predictions. (6) Lack of multi-modal biomarkers: the model only integrates serum KCP and clinical factors, and the inclusion of additional molecular biomarkers (e.g., circulating tumor DNA, radiomic features) may improve predictive performance.

Future research will focus on the following aspects: (1) expanding the sample size through multi-center prospective cohort studies to optimize the nomogram and improve its external validity [27,32]; (2) exploring the molecular mechanism of KCP-mediated paclitaxel resistance through in vitro and in vivo experiments, with emphasis on the TGF-β1/BMP/EMT signaling axis [24,25]; (3) experimentally validating the top-ranked candidate compounds identified by DrugReflector through in vitro drug sensitivity assays and in vivo xenograft models; (4) integrating KCP with other promising biomarkers (e.g., circulating tumor DNA, radiomic features) to construct a multi-modal predictive model with higher accuracy [33]; (5) standardizing the detection method of serum KCP and developing a clinical detection kit; and (6) conducting long-term follow-up to further evaluate the prognostic value of KCP.

Conclusion

This study identified KCP as a novel potential serum biomarker for paclitaxel resistance in advanced cervical cancer, with an optimal cutoff value of 24.59 ng/L demonstrating good predictive ability for chemotherapy resistance. The KCP-integrated nomogram achieved moderate discriminatory ability in the training cohort (AUC = 0.738) but exhibited poor external validity in prospective validation (AUC = 0.535), highlighting the limitations of single-center retrospective model construction and the necessity of prospective external validation. Computational drug virtual screening using DrugReflector identified 9,597 candidate compounds that may potentially reverse KCP-mediated chemoresistance, providing a foundation for future therapeutic development. These findings support the clinical value of KCP in pre-treatment screening of paclitaxel-resistant cervical cancer patients and emphasize that multi-center prospective design, standardized data collection, and integration of specific molecular biomarkers are essential for optimizing chemotherapy resistance predictive models. Future research will focus on mechanistic exploration, experimental validation of candidate drugs, and multi-center validation to promote the clinical translation of KCP and improve precision treatment for advanced cervical cancer.

Abbreviations

KCP: Kielin/chordin-like protein

ELISA: Enzyme-linked immunosorbent assay

IHC: Immunohistochemistry

TGF-β1: Transforming growth factor β1

BMP: Bone morphogenetic protein

SCCA: Squamous cell carcinoma antigen

ROC: Receiver operating characteristic

AUC: Area under the curve

PFS: Progression-free survival

OS: Overall survival

DCA: Decision curve analysis

EMT: Epithelial–mesenchymal transition

LVSI: Lymphovascular space invasion

NACT: Neoadjuvant chemotherapy

FIGO: International Federation of Gynecology and Obstetrics

RECIST: Response Evaluation Criteria in Solid Tumors

CR: Complete response

PR: Partial response

SD: Stable disease

PD: Progressive disease

HR: Hazard ratio

CI: Confidence interval

TISCH: Tumor Immune Cell Atlas

Declarations

Acknowledgments

We thank all the reviewers and editors who provided comments that helped to substantially improve the manuscript. We thank Beijing Municipal Science and Technology Commission, National Natural Science Foundation of China, Beijing Hospitals Authority Clinical Medicine Development of Special Funding Support , for supporting our research.

Author Contributions

Conceptualization, H.Y. and W.Y.M.; Methodology, J.C.; Investigation, W.Y. and L.Y.; Data curation, H.Y.; Formal analysis, J.C.& X.M.R.; Writing—original draft, J.C.; Writing—review & editing, H.Y.; Supervision, L.C.Y.; Funding acquisition, H.Y.& W.Y.M. All authors have read and agreed to the published version of the manuscript.

Conflicts of Interest

The authors declare that they have no known competing financial interests or personal relationships that could have appeared to influence the work reported in this paper.

Data availability statement

The datasets used and/or analysed during the current study available from the corresponding author on reasonable request.

Fundings

This work was supported by the Beijing Municipal Science and Technology Commission (Z221100007422087), National Natural Science Foundation of China (82102711), Beijing Hospitals Authority Clinical Medicine Development of Special Funding Support (ZLRK202529).

Statement of experiments on human tissue samples

All human subject procedures strictly followed the Declaration of Helsinki. All methods were carried out in accordance with relevant guidelines and regulations. The study was approved by the Ethics Committee of Beijing Obstetrics and Gynecology Hospital, Capital Medical University (Ethics Approval No. 2023-KY-003-02), and written informed consent was obtained from all enrolled participants.

References

1. Benedict NL, et al. Cervical cancer screening practices among women in Ghana: evidence from wave 2 of the WHO study on global AGEing and adult health. BMC Womens Health. 2020;20(1):49.
2. Bray F, Laversanne M, Sung H, et al. Global cancer statistics 2022: GLOBOCAN estimates of incidence and mortality worldwide for 36 cancers in 185 countries. CA Cancer J Clin. 2024;74(3):229–63.
3. Duan R, et al. Cancer burden attributable to human papillomavirus infection by sex, cancer site, age, and geographical area in China. Cancer Med. 2020;9(1):374–84.
4. Arbyn M, et al. Estimates of incidence and mortality of cervical cancer in 2018: a worldwide analysis. Lancet Glob Health. 2020;8(2):e191–203.
5. Marabelle A, et al. Pembrolizumab plus chemotherapy versus chemotherapy alone for first-line treatment of advanced cervical cancer (KEYNOTE-826): a randomised, double-blind, phase 3 trial. Lancet. 2021;398(10302):797–808.
6. Monk BJ, et al. Cemiplimab plus chemotherapy versus chemotherapy alone for recurrent or metastatic cervical cancer (BEATcc): a randomised, phase 3 trial. Lancet Oncol. 2023;24(1):39–50.
7. He Y, Xu J-Q, Wang Y, et al. Examination of the functions and mechanism of KCP in mediating paclitaxel resistance in cervical squamous carcinoma cells. Front Oncol. 2025;15:1550032. 10.3389/fonc.2025.1550032.
8. Rydzewska L, et al. Neoadjuvant chemotherapy for locally advanced cervical cancer. Cochrane Database Syst Rev. 2012;4:CD007510.
9. Puy LA, Lo CG, Olcese JE, et al. Analysis of a 24-kilodalton (KD) protein in the human uterine cervix during abnormal growth. Cancer. 1989;64(5):1067–73.
10. Liu J, Liu J, Li SZ, et al. Inhibition of heat shock protein 70 expression enhances the chemosensitivity of cervical cancer cells to cisplatin. J South Med Univ. 2017;37(4):475–81.
11. Huang Z, Zhang S, Shen Y, et al. Influence of MDR1 methylation on the curative effect of interventional embolism chemotherapy for cervical cancer. Ther Clin Risk Manag. 2016;12:217–23.
12. Xiao J, Zhou J, Liang L, et al. Sensitivity of ASPP and P-gp to neoadjuvant chemotherapy combined with gene therapy in locally advanced cervical cancer. J BUON. 2019;24(3):967–74.
13. Wada T, Fukuda T, Shimomura M, et al. XPA expression is a predictive marker of the effectiveness of neoadjuvant chemotherapy for locally advanced uterine cervical cancer. Oncol Lett. 2018;15(3):3766–71.
14. Soofi A, et al. The kielin/chordin-like protein (KCP) attenuates high-fat diet-induced obesity and metabolic syndrome in mice. J Biol Chem. 2017;292(22):9051–62.
15. Soofi A, et al. Kielin/chordin-like protein attenuates both acute and chronic renal injury. J Am Soc Nephrol. 2013;24:897–905.
16. Liu Z, Zhang Y, Zhang L, et al. Duality of interactions between TGF-β and TNF-α during tumor formation. Front Immunol. 2021;12:810286.
17. Fukuda T, Fukuda R, Miyazono K et al. Tumor promoting effect of BMP signaling in endometrial cancer. Int J Mol Sci. 2021;22(15).
18. Ye J, Wang Z, Wang M, et al. Increased kielin/chordin-like protein levels are associated with the severity of heart failure. Clin Chim Acta. 2018;486:381–6.
19. Zannoni GF, Travaglino A, Raffone A, et al. Depth of stromal invasion as the most prognostically relevant regression system in locally advanced cervical cancer after neoadjuvant treatment: a systematic review and meta-analysis grading. Diagnostics (Basel). 2021;11(10):1772. 10.3390/diagnostics11101772.
20. Zhang Y, Liu X, Chen J, et al. Predictive value of combined SCC-Ag and miR-21 detection for neoadjuvant chemotherapy efficacy in locally advanced cervical cancer. Gynecol Oncol. 2021;161(2):462–8. 10.1016/j.ygyno.2021.02.018.
21. Li L, Wu L, Wang Y et al. Development of a venous thromboembolism risk prediction model for patients with primary membranous nephropathy based on machine learning. Front Pharmacol. 16:1683708.
22. Han M, Yang X, Li J, et al. KCP promotes gastric cancer progression by regulating the TGF-β1/Smad3 signaling pathway. Oncotarget. 2023;14(5):489–502. 10.18632/oncotarget.28976.
23. Manso L, Ramchandani-Vaswani A, Romero I, et al. SEOM-GEICO clinical guidelines on cervical cancer (2023). Clin Transl Oncol. 2024;26(11):2771–82.

24. Chen L, Zhang H, Wang Y, et al. TGF-β1-induced epithelial–mesenchymal transition mediates paclitaxel resistance in cervical cancer cells via upregulating ABCB1. Cell Death Dis. 2022;13(8):721. 10.1038/s41419-022-05109-8.
25. Li S, Zhao J, Hu X, et al. BMP signaling inhibits paclitaxel resistance in cervical cancer by suppressing EMT through the Smad1/5/8 pathway. Int J Mol Sci. 2024;25(3):1689. 10.3390/ijms25031689.
26. Ryu JH, Kim JH, Park ST, et al. Preoperative SCCA as a predictor of parametrial invasion and lymph node metastasis in early-stage cervical squamous cell carcinoma. Gynecol Oncol. 2016;141:245–50.
27. Collins GS, et al. External validation of multivariable prediction models: a systematic review of methodological conduct and reporting. BMC Med Res Methodol. 2014;14:40. 10.1186/1471-2288-14-40.
28. Siontis GCM, et al. External validation of new risk prediction models is infrequent and reveals worse prognostic discrimination. J Clin Epidemiol. 2015;68(1):25–34. 10.1016/j.jclinepi.2014.07.013.
29. Queiroz ACM, Fabri V, Mantoan H, et al. Risk factors for pelvic and distant recurrence in locally advanced cervical cancer. Eur J Obstet Gynecol Reprod Biol. 2019;235:6–12.
30. Wang J, Liu Z, Zhang Q, et al. Clinicopathological risk factors for recurrence in locally advanced cervical cancer after neoadjuvant chemotherapy and radical surgery. Eur J Gynaecol Oncol. 2021;42(6):987–92.
31. Yang Q, Han X, et al. Prognostic value of risk factors in cervical squamous cell carcinoma based on tumour infiltration depth. BMC Cancer. 2025;25(1):1412.
32. Qin S, Wang Y, Ma C, et al. Competitive endogenous network of circRNA, lncRNA, and miRNA in osteosarcoma chemoresistance. Eur J Med Res. 2023;28(1):354.
33. Wang W, Yang G, Liu Y, et al. Multimodal deep learning model for prognostic prediction in cervical cancer receiving definitive radiotherapy: a multi-center study. npj Digit Med. 2025;8:503.

Figures

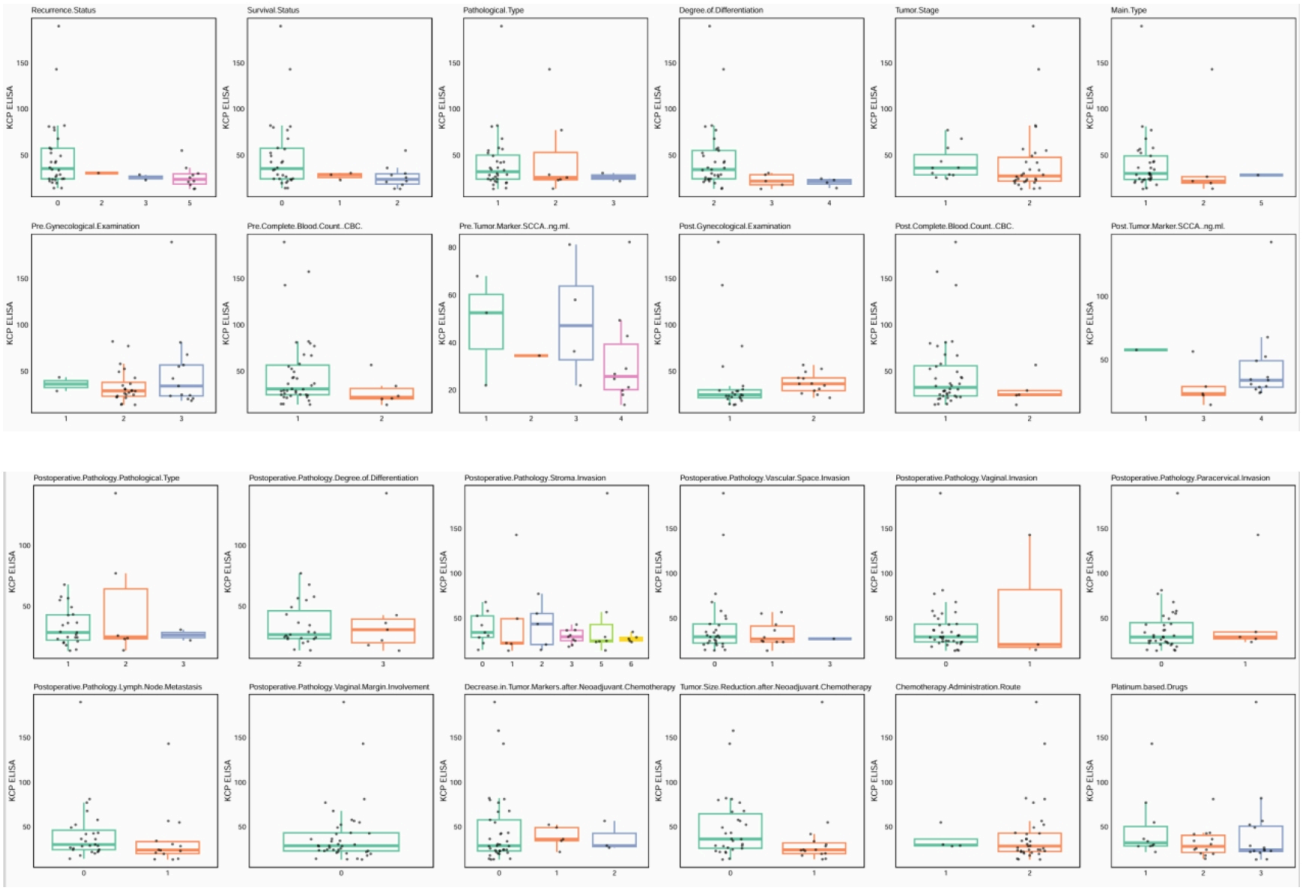


Figure 1

Risk factors affecting recurrence of advanced cervical cancer after neoadjuvant chemotherapy in the training cohort. (A) Forest plot of univariate Cox regression analysis. (B) Forest plot of multivariate Cox regression analysis.

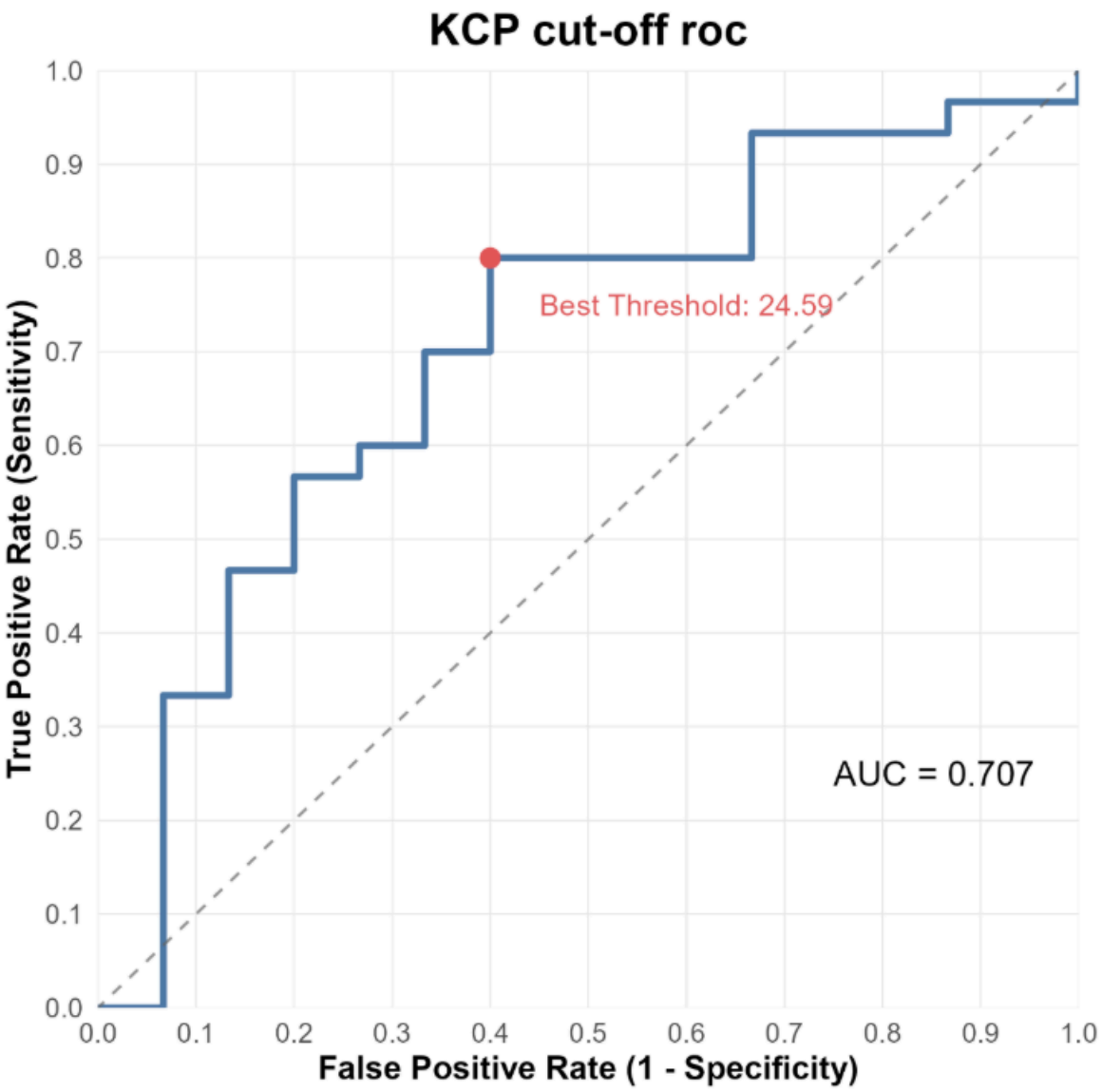


Figure 2

ROC curve of serum KCP for predicting chemoresistance in cervical cancer in the training cohort.

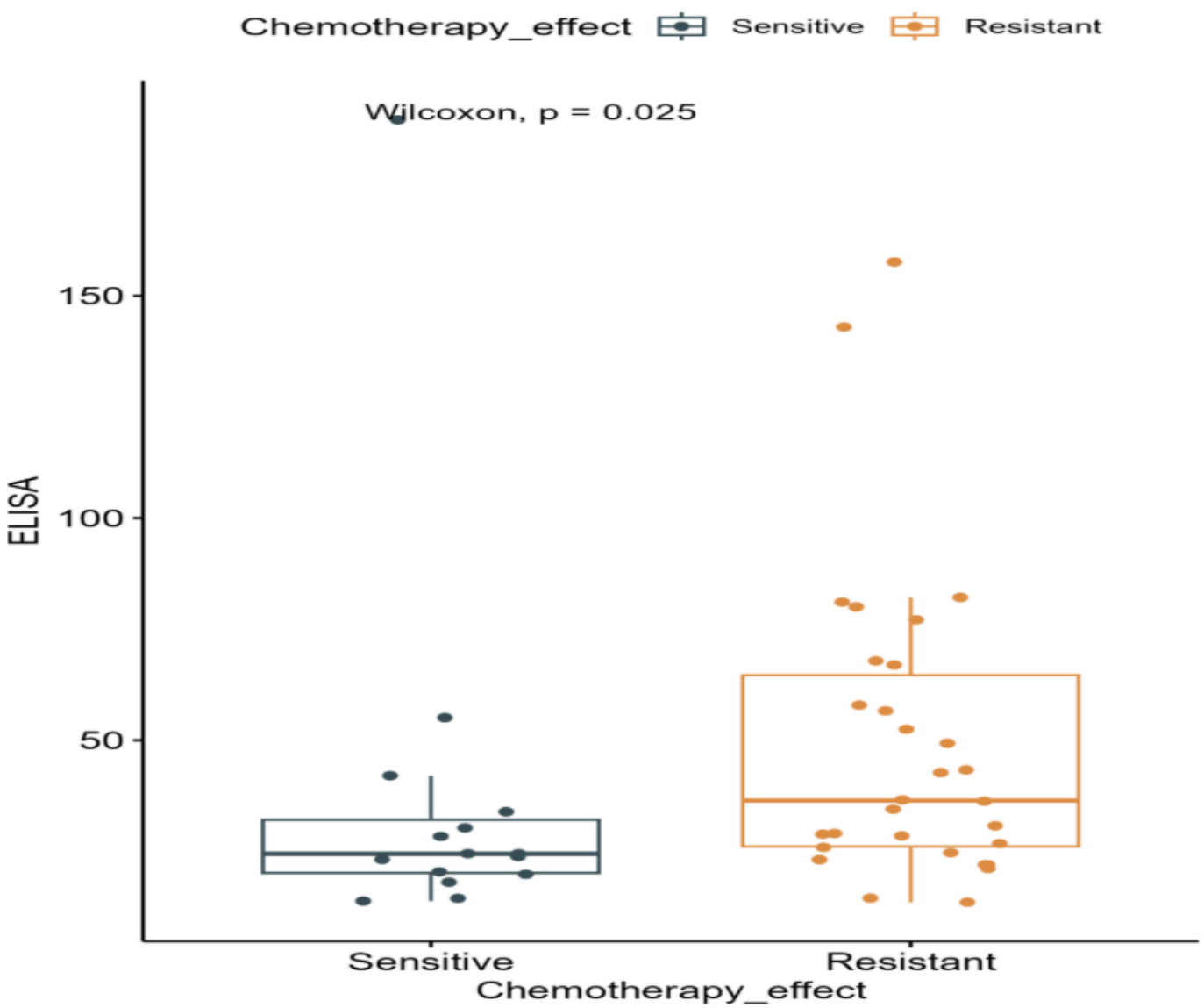


Figure 3

Association between serum KCP levels and chemoresistance in the training cohort. Boxplot comparing KCP levels between chemosensitive (S) and chemoresistant (R) groups.

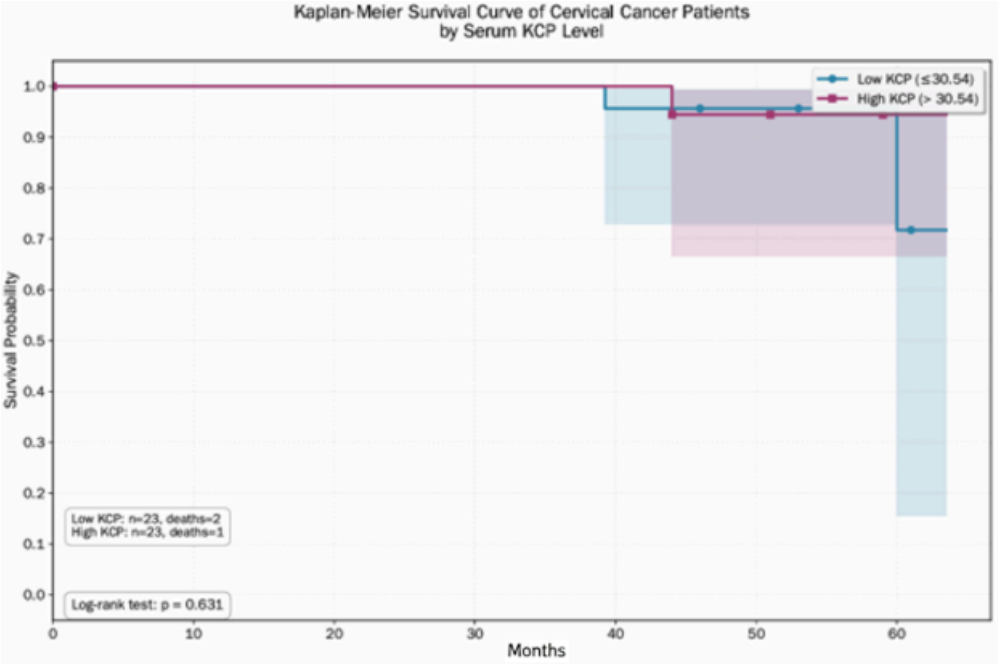


Figure 4

Kaplan–Meier survival curve stratified by serum KCP level in the training cohort.

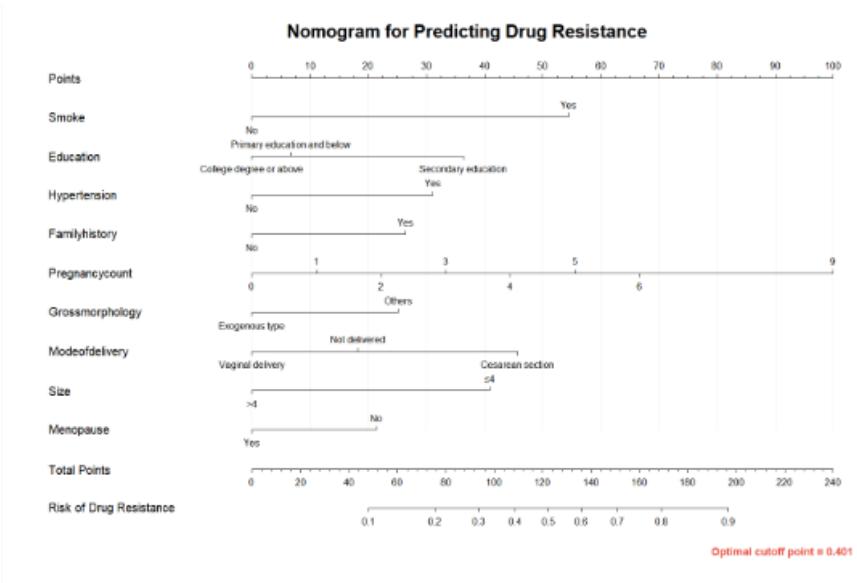


Figure 5

Figure 5.1. Nomogram for predicting chemoresistance based on clinical factors.

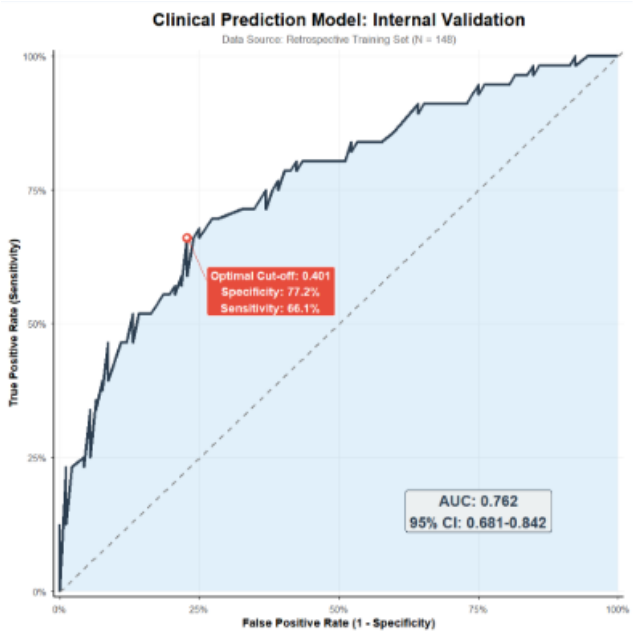


Figure 6

Figure 5.2. ROC curve for evaluating the reliability of the clinical factor-based nomogram.

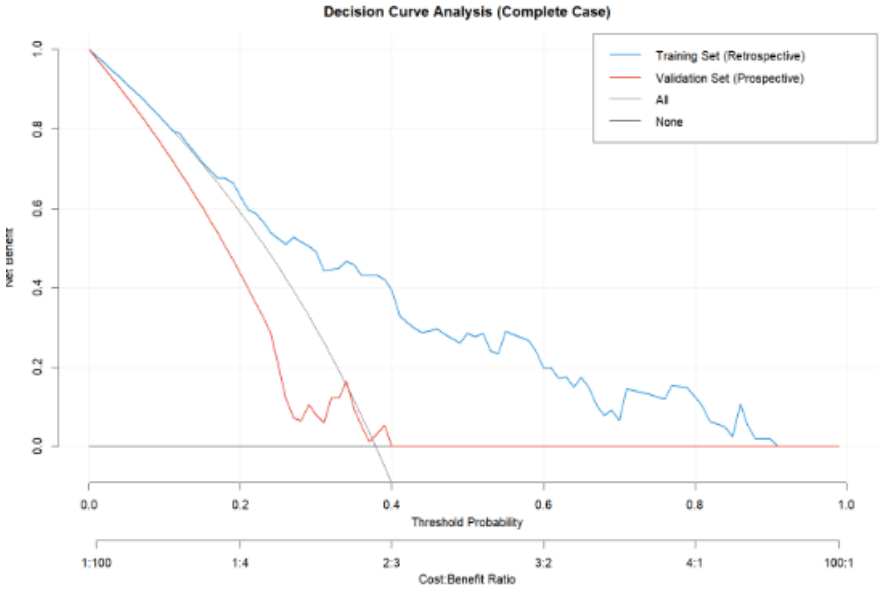


Figure 7

Figure 6. Decision curve analysis evaluating the clinical net benefit of the chemotherapy resistance prediction model across different threshold probabilities in the training (A) and validation (B) cohorts.

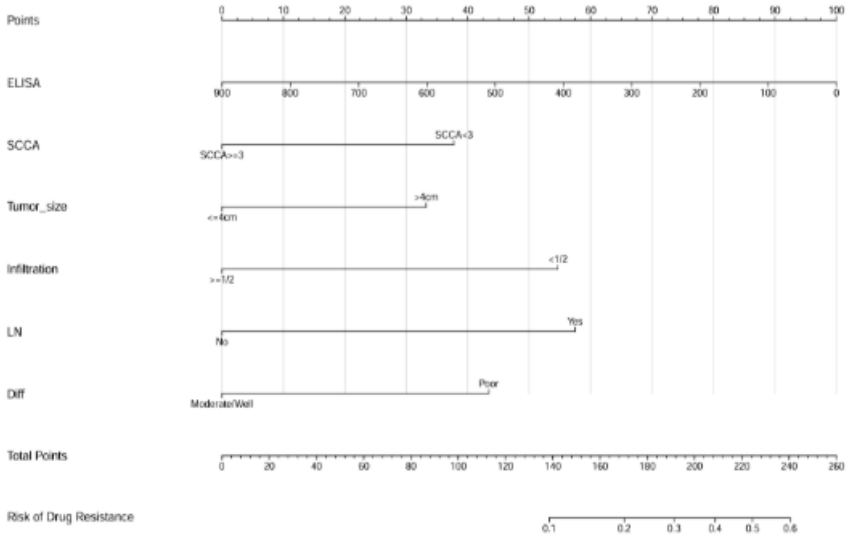


Figure 8

Figure 7.1. KCP-integrated nomogram for predicting chemotherapy response.

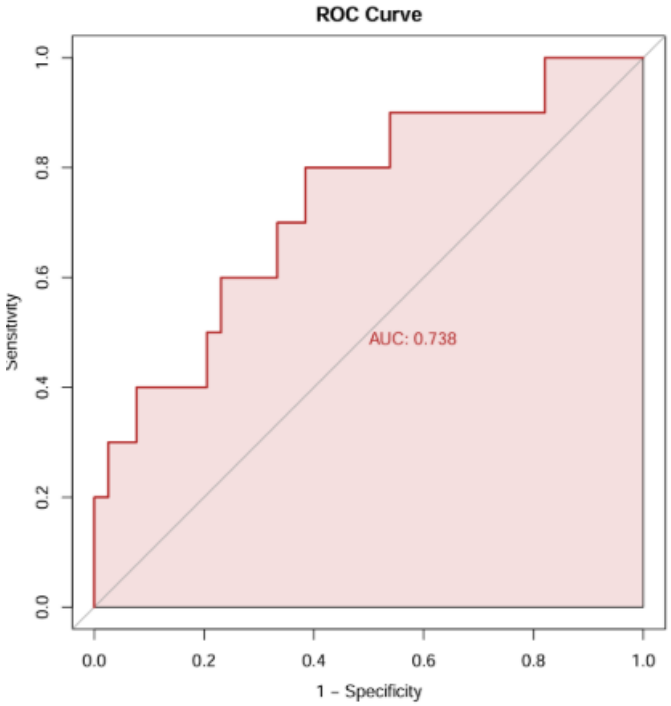


Figure 9

Figure 7.2. ROC curve evaluating the predictive performance of the KCP-integrated nomogram for chemotherapy outcomes in cervical cancer.

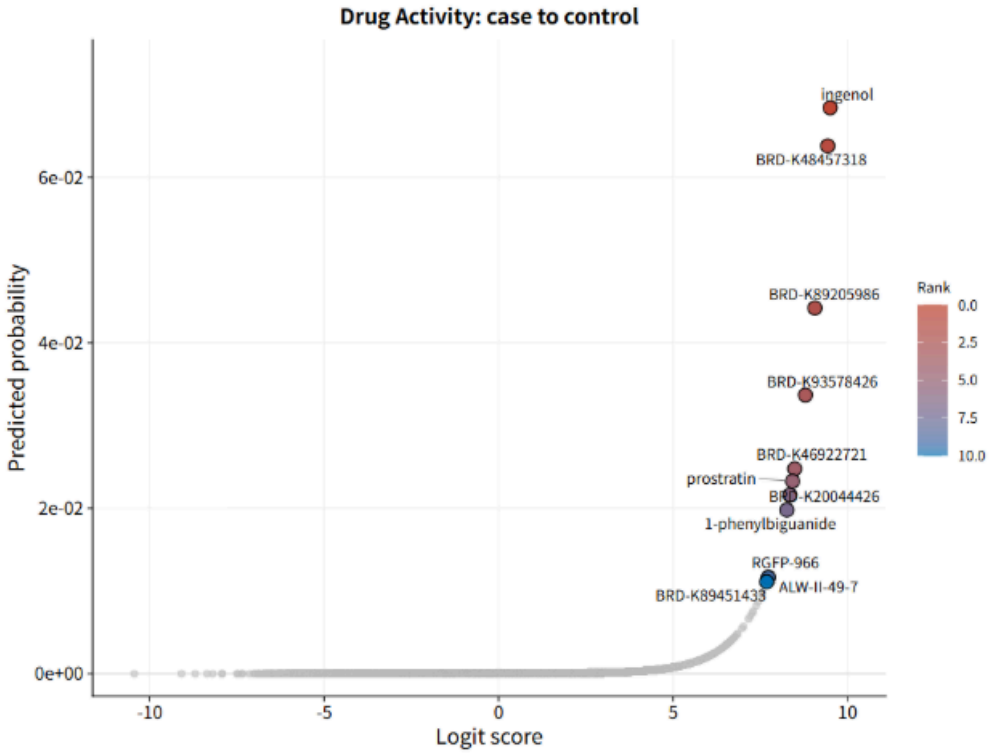


Figure 10

Figure 8. Drug virtual screening results from DrugReflector. Each point represents a candidate compound predicted by DrugReflector. The x-axis indicates the model logit score, and the y-axis indicates the predicted probability. Highlighted and labeled points represent the top-ranked candidate drugs. Color denotes drug rank, with blue indicating higher-ranked candidates and red indicating relatively lower-ranked candidates among the displayed compounds.